Basic and Clinical NEUROSCIENCE

November & December 2025, Vol 16, No. 6

Research Paper

Neuroprotective Effects of Astaxanthin After Middle Cerebral Artery Occlusion Stroke in Male Rats: The CA1 Hippocampal Region

Parsa Pourmohammadi[1], Mobina Gheibi[2, 3], Sina Baghi Keshtan[4], Erfan Ghadirzadeh[3], Melika Pourhossein[5], Ali Siahposht-Khachaki[6*]

1. Animal Research Center, Mazandaran University of Medical Sciences, Sari, Iran.
2. Department of Laboratory Sciences, Razi Hospital, Mazandaran University of Medical Sciences, Qaemshahr, Iran.
3. Non-communicable Diseases Institute, Mazandaran University of Medical Sciences, Sari, Iran.
4. School of Medicine, Birjand University of Medical Sciences, Birjand, Iran.
5. Faculty of Pharmacy, Mazandaran University of Medical Sciences, Sari, Iran.
6. Department of Physiology, Immunogenetics Research Center, Faculty of Medicine, Mazandaran University of Medical Sciences, Sari, Iran.

Use your device to scan and read the article online

Citation Pourmohammadi, P., Gheibi, M., Baghi Keshtan, S., Ghadirzadeh, E., Pourhossein, M., & Siahposht-Khachaki, A. (2025). Neuroprotective Effects of Astaxanthin After Middle Cerebral Artery Occlusion Stroke in Male Rats: The CA1 Hippocampal Region. *Basic and Clinical Neuroscience, 16*(6), 1143-1158. http://dx.doi.org/10.32598/bcn.2025.7494.2

http://dx.doi.org/10.32598/bcn.2025.7494.2

Article info:
Received: 10 Jul 2025
First Revision: 26 Aug 2025
Accepted: 02 Oct 2025
Available Online: 01 Nov 2025

Keywords:
Astaxanthin (ATX), Middle cerebral artery occlusion (MCAO), Reperfusion injury, Rat, Ischemic stroke

ABSTRACT

Introduction: Ischemic stroke often results in severe neurological impairment, particularly affecting the hippocampal CA1 region, which is highly vulnerable to ischemia-reperfusion injury. Astaxanthin (ATX), a potent antioxidant carotenoid, exhibits neuroprotective, anti-inflammatory, and anti-apoptotic properties. This study aimed to investigate the effects of ATX on functional, biochemical, and histological outcomes in a focal transient middle cerebral artery occlusion (MCAO) model in rats.

Methods: Fifty-six male Wistar rats were randomly assigned to seven groups: Intact, sham, stroke (MCAO), solvent (0.1% dimethyl sulfoxide [DMSO]), and ATX-treated groups (25, 50, or 100 mg/kg, intraperitoneally every 12 hours for 3 days post-MCAO). Neurological function (Bederson score), motor coordination (rotarod), spatial learning (Morris water maze [MWM]), and memory retention (passive avoidance learning [PAL] using shuttle box) were assessed. Cerebrospinal fluid (CSF) cytokine levels (interleukin [IL]-10, IL-1β), cerebral edema, and hippocampal CA1 histology were analyzed.

Results: Low (25 mg/kg) and medium (50 mg/kg) ATX doses significantly improved neurological and functional performance compared with untreated MCAO rats ($P<0.01$). These doses increased IL-10, reduced IL-1β levels, decreased brain water content, and preserved neuronal morphology in the CA1 region. Conversely, the high dose (100 mg/kg) conferred no significant benefits. Histopathology confirmed reduced neuronal damage and apoptosis at effective doses.

Conclusion: Post-ischemic ATX administration provides neuroprotection in a rat MCAO model, with 25–50 mg/kg yielding optimal outcomes. The observed inverted dose-response underscores the importance of precise dosing and timing. ATX represents a promising therapeutic candidate for ischemic stroke pending further translational studies.

*** Corresponding Author:**
Ali Siahposht-Khachaki, Associate Professor.
Address: *Department of Physiology, Immunogenetics Research Center, Faculty of Medicine, Mazandaran University of Medical Sciences, Sari, Iran.*
Tel: *+98 (911) 1206800*
E-mail: *ak57n@yahoo.com, a.siahposht@mazums.ac.ir*

Highlights

- ATX (25 and 50 mg/kg) improved neurological function post-stroke.
- Low and medium doses reduced cerebral edema and neuroinflammation.
- The effective doses preserved hippocampal CA1 neuronal structure.
- A high dose (100 mg/kg) showed no neuroprotective benefits.

Plain Language Summary

A stroke occurs when the blood supply to part of the brain is cut off, which can cause lasting brain damage, disability, and problems with memory and movement. The hippocampus, a specific part of the brain, is especially vulnerable to this type of damage. In this study, researchers investigated whether natural substance astaxanthin (ATX) could protect the brain after a stroke. ATX is a powerful antioxidant found in seafood, such as salmon, and in microalgae, and is known for its anti-inflammatory properties. The study was conducted on male rats that had experienced an experimentally induced stroke. We treated the rats with different doses of ATX after stroke. Then, we measured the rats' recovery by examining their ability to move, learn, and remember, as well as brain swelling and inflammation. We found that rats given low and medium doses of ATX (25 and 50 mg/kg) showed significant improvements. These animals exhibited improved memory and coordination, reduced brain swelling, and reduced inflammation. Brain cells in the critical hippocampal region were also better preserved. Surprisingly, a higher dose (100 mg/kg) provided no benefit. This research is crucial because stroke is a leading cause of disability worldwide, and treatment options are limited. The findings suggest that ATX could be a promising candidate for a new stroke therapy, helping to protect the brain from damage and improve recovery. However, the discovery that a higher dose was ineffective is a critical warning; it shows that "more is not always better." This emphasizes the need for careful future studies to determine the perfect dose and timing for treatment in humans, ensuring this potential therapy is both safe and effective.

Introduction

Of all stroke types, ischemic stroke, triggered by a blockage in a cerebral blood vessel, is the most common and a major contributor to global mortality and disability (Saini et al., 2021). The middle cerebral artery (MCA) is frequently occluded in such events, often resulting in serious neurological impairment. A brain area especially susceptible to this damage is the CA1 region of the hippocampus, owing to its high metabolic rate and sensitivity to interruptions in oxygen and glucose (Liang et al., 2016; Zhu et al., 2012). This sensitivity can lead to significant cognitive and behavioral deficits, making the CA1 a key focus for research on neuroprotection after stroke.

A paradoxical phenomenon known as ischemia-reperfusion injury can worsen cellular damage when blood flow is restored (for instance, by tissue plasminogen activator) (Jurcau & Ardelean, 2022). This process accelerates the formation of reactive oxygen species (ROS), leading to oxidative stress, mitochondrial dysfunction, and the activation of complex neurotoxic cascades involving excitotoxicity, inflammation, and apoptosis. The resulting neuroinflammation, driven by pro-inflammatory cytokines, such as tumor necrosis factor alpha (TNF-α), interleukin (IL)-6, and IL-1β, disrupts the blood-brain barrier (BBB), exacerbates edema, and contributes to secondary neuronal death (Jurcau & Ardelean, 2022; Sun et al., 2018). Therefore, therapeutic agents that can simultaneously mitigate oxidative stress, inflammation, and apoptotic pathways are of immense interest (Lin et al., 2016; Mahyar et al., 2025).

Astaxanthin (ATX), a naturally occurring xanthophyll carotenoid found in microalgae and seafood, has emerged as a potent candidate. It is a powerful antioxidant, with a molecular structure that allows it to effectively quench free radicals and protect cell membranes. Beyond its antioxidant capacity, ATX has demonstrated significant anti-inflammatory and anti-apoptotic properties in various experimental models of liver, retina, and kidney ischemia-reperfusion injury (Li et al., 2017; Otsuka et al., 2016; Qiu et al., 2015). Its neuroprotective potential has been observed in studies of global cerebral ischemia and subarachnoid hemorrhage, where it acti-

vates protective cellular pathways such as the nuclear factor erythroid 2-related factor 2 (Nrf2)/ antioxidant response element (ARE) signaling cascade, leading to the upregulation of endogenous antioxidant enzymes, such as heme oxygenase-1 (HO-1) (Ashrafizadeh et al., 2022; Qian et al., 2021; Taheri et al., 2022; Xue et al., 2017; Yang et al., 2021; Yuguang et al., 2025). Critically, ATX is fat-soluble, enabling it to cross the BBB, and has an established safety profile with approval for use as a dietary supplement (Brendler & Williamson, 2019; Galasso et al., 2018; Grimmig et al., 2017).

However, despite these promising attributes, its specific effects on regional brain ischemia, particularly on the vulnerable hippocampal CA1 neurons following focal MCAO, remain insufficiently explored. The existing evidence highlights a need to elucidate the precise behavioral, biochemical, and histological outcomes associated with ATX treatment in a focal stroke model. Consequently, this study aimed to determine whether ATX provides neuroprotection, specifically for hippocampal CA1 neurons, in an MCAO rat model by evaluating its effects on functional recovery through behavioral tests, quantifying the modulation of key inflammatory markers (ILs), and assessing the preservation of neuronal structure through qualitative histopathological analysis.

Materials and Methods

Animals

This experiment utilized 56 male Albino-Wistar rats, weighing 250-300 g and aged 8-10 weeks. The animals were kept in a controlled environment with a 12-hour light/dark cycle, a temperature range of 22-25 ˚C, and unrestricted access to food and water. The Research Ethics Committee of Laboratory Animals at Mazandaran University of Medical Sciences granted ethical approval for all procedures. The study adhered to the animal research: Reporting of in vivo experiments (ARRIVE) guidelines, the university's ethical standards, and the UK's Animals (Scientific Procedures) Act 1986.

Experimental groups

Figure 1 shows a schematic of the study's experimental protocol. The rats were randomly divided into the following seven experimental groups (eight rats each):

Intact group: No intervention.

Sham group: Surgery and anesthesia without MCAO induction.

Stroke group: MCAO was induced, but the patients received no medication or placebo.

Solvent group: MCAO + 0.1% dimethyl sulfoxide (DMSO) (as solvent or placebo)

Low-dose group: MCAO + 25 mg/kg ATX

Medium-dose group: MCAO + 50 mg/kg ATX

High-dose group: MCAO + 100 mg/kg ATX

All the injections were administered intraperitoneally (IP) 30 minutes after stroke induction and were repeated every 12 hours for up to 3 days (6 total doses after MCAO induction).

Inclusion criteria

Animals demonstrating neurological deficits in pretests that were indicative of a successful MCAO procedure (in groups induced by stroke).

Exclusion criteria

Subjects who failed the initial pretest assessments.

Those that did not develop observable neurological deficits following stroke induction, suggesting an unsuccessful MCAO.

Animals experiencing major non-neurologic post-surgical sequel, such as infection or bleeding, which could compromise their well-being and skew experimental outcomes.

Any participants who died prior to the scheduled conclusion of the study.

Low motivation for the dark room in the shuttle box test (step-through latency [STL] duration exceeds 60 seconds)

Middle cerebral artery occlusion (MCAO) induction model

Focal cerebral ischemia was induced using the transient intraluminal filament MCAO (tifMCAO) model, as previously described (Mahyar et al., 2025; Themistoklis et al., 2022). Briefly, Wistar rats (300–400 g) were anesthetized with isoflurane and placed supine on a heating pad to maintain body temperature at ~37 ˚C. A midline or right paramedian neck incision (~2–3 cm) was made. The common carotid artery (CCA), external carotid ar-

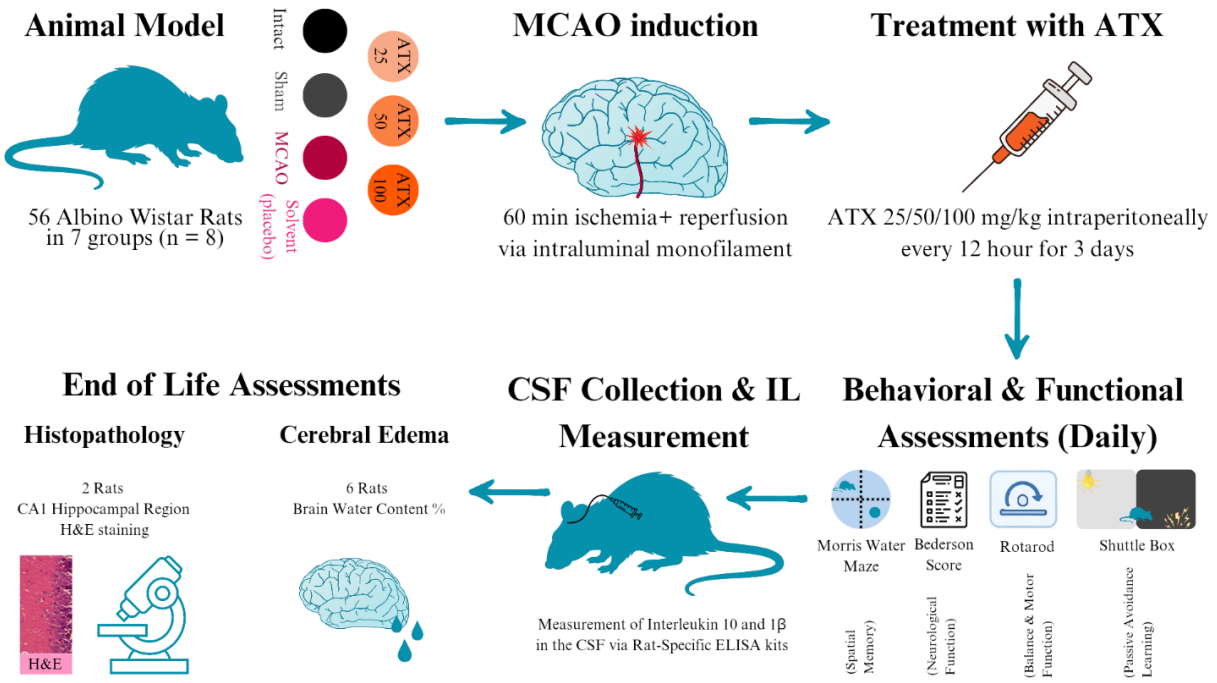

Figure 1. Schematic outline of the study's experimental protocol

NEUROSCIENCE

Note: Fifty-six male rats were randomly assigned to one of seven experimental groups. The intact and sham groups underwent neither stroke induction nor pharmacological intervention. The MCAO group received the stroke induction procedure without any drug treatment, and the solvent group, in addition to MCAO, was administered an intraperitoneal injection of DMSO as a vehicle control (with the same intervals as the ATX groups). Three treatment groups were given intraperitoneal injections of ATX at dosages of 25, 50, or 100 mg/kg. The first dose was administered 30 minutes after the stroke induction, with subsequent doses given every 12 hours for a total of 3 days. All animals were assessed daily using a range of neurobehavioral and functional tests, including the Bederson neurological score, rotarod balance test, shuttle box passive avoidance test, and the MWM memory test. After this testing period, CSF was collected from each rat for cytokine evaluation prior to euthanasia. Brain tissue was then harvested; two brains from each group were designated for qualitative histopathological analysis with H&E staining, and the remaining six were used to quantify cerebral edema percentage.

tery (ECA), and internal carotid artery (ICA) were carefully exposed through microsurgical dissection. The superior thyroid artery and occipital artery were coagulated and divided. A complete arteriotomy of the ECA stump was performed. Temporary clips were placed on the CCA and ICA, and a silicone-coated nylon monofilament (diameter ~0.28–0.38 mm) was introduced through the ECA stump and advanced intracranially along the ICA approximately 18–20 mm until resistance was felt, indicating occlusion of the middle cerebral artery origin. After 60 minutes of occlusion, the filament was withdrawn to allow reperfusion. The ECA stump was permanently ligated, the wound was closed in layers, and the animals were allowed to recover with postoperative monitoring and analgesia.

Neurological function assessment

Neurological function was assessed daily for three days according to the Bederson scale (Bieber et al., 2019), graded from 0 to 5 as follows: 0, no deficit; 1, forelimb flexion; 2, forelimb flexion combined with reduced resistance when pushed laterally; 3, circling to one side; 4, circling accompanied by a depressed level of consciousness; and 5, death or a state of unresponsiveness and immobility.

Motor coordination and balance assessment

To evaluate motor coordination and balance in the rats, a rotarod apparatus (Model 6700 MT, Borjsanat Company, IR) was employed each day following MCAO induction. The equipment consists of a rotating rod capable of speeds from 0 to 40 rpm. Prior to testing, the animals were acclimated to the device by being placed on the rod rotating at 10 rpm with an acceleration rate of 7 rpm². One hour after ATX administration, the animals were placed on the rotarod, and the latency to fall was recorded, with a maximum cutoff time set at 300 s.

Spatial learning, memory, and visual-motor abilities

Spatial learning and memory capabilities were evaluated daily after MCAO induction using the morris water maze (MWM) (Nunez, 2008; Othman et al., 2022). The apparatus consisted of a circular water tank (140 cm in diameter, 55 cm high) filled with water (20±1 ˚C) to a depth of 25 cm and divided in four imaginary quadrants. A submerged platform (11 cm in diameter), hidden 1 cm beneath the water's surface, was positioned in the center of one quadrant (target quadrant). All trials were video-recorded and analyzed with EthoVision XT 10.1 software (Noldus Information Technology, Netherlands) to quantify swimming velocity and the percentage of time spent in the target quadrant. Twenty-four hours prior to formal training, rats were allowed a 1-minute habituation period in the pool without the platform. The training phase spanned two consecutive days, with four trials per day. During these trials, the platform remained stationary in its designated quadrant. For each trial, a rat was released from one of four randomized start locations (north, south, east, or west) facing the wall. The trial concluded when the animal located the platform or after 60 s. A 50-second inter-trial rest period was provided, comprising 20 s on the platform and 30 seconds in a dry cage. Animals that failed to find the platform within the time limit were gently guided to it. Following the trials, the rats were dried and returned to their home cages. A probe test (recall test) was administered 24 hours after the final training session. The platform was removed, and each rat was released from a novel starting point. Their behavior was tracked for 60 s to measure the duration spent in the target quadrant. Fifteen minutes later, a visible platform test was conducted, where the platform, marked with aluminum foil, was placed in a different quadrant. This test was used to control for potential effects of the treatment on visual-motor function and motivation.

Passive avoidance learning (PAL) assessment

PAL test was conducted daily after MCAO induction using a shuttle box apparatus, and the mean results were compared between groups. The shuttle box apparatus was constructed from Plexiglass, divided into two equal-sized compartments (20×40×20 cm). These sections differed in illumination: One was brightly illuminated by a 100-watt overhead lamp, and the other was kept dark. The compartments were separated by a guillotine door measuring 5.7×5.7 cm. Both sections featured a floor made of 2-mm stainless steel rods spaced 1 cm apart. The floor in the dark compartment was wired to an electrical stimulator to administer a predefined foot shock to the subjects. The PAL test was conducted following a three-phase protocol:

Acclimatization: To habituate the animals to the apparatus, they were placed in an illuminated compartment. After 10 seconds, the guillotine door was raised. The door was closed once the animal's hind legs fully entered the dark compartment. Following a 30-second interval in the dark, the animal was returned to its home cage. This procedure was repeated after a 30-minute delay. The STL, defined as the time taken to move from the light to the dark chamber during this phase, was recorded. Animals exhibiting an step-through latency (STL) greater than 60 seconds were excluded from the study due to insufficient innate preference for the dark environment.

Training (acquisition): The training trial commenced 30 minutes after the second acclimatization. The animals were again placed in the light chamber. After 10 seconds, the door was opened. Upon entry into the dark section, the door was closed, and a foot shock (1 Ampere, 50 Hz, and 1.5 s duration) was delivered. The animal was removed after 20 seconds. Two minutes later, it was returned to the light chamber for a retention test; a successful PAL outcome was defined as refusing to enter the dark compartment within 120 seconds after the door was opened. If the animal re-entered, the door was closed and the shock was repeated. The number of such training trials required was recorded for each subject.

Recall test: Memory retention was evaluated 24 hours post-training. The animal was positioned in the light compartment, and the door was opened after a 10-second delay. During a 300-second observation period, the STL, the total time spent in the illuminated compartment, and the number of entries into the dark chamber were documented. For the statistical analysis in this investigation, the STL and the time spent in the light compartment were the primary measures utilized.

These measurements evaluate learning and memory retention by quantifying the animal's success in remembering and evading the context where an aversive foot shock was administered.

Measurement of cytokines in the cerebrospinal fluid (CSF)

At the end of the three-day duration of behavioral tests, rats were first anesthetized using ketamine (50 mg/kg) and xylazine (10 mg/kg), then secured in a stereotaxic apparatus after shaving the posterior neck area. With the head angled at 45 degrees, a 200 µL sample of CSF was withdrawn from the cisterna magna using a Hamilton syringe and polyethylene tubing, as described in a previous study (Shimizu et al., 2022). To prevent hemo-contam-

ination, the fluid was aspirated carefully. The collected CSF was immediately placed in an Eppendorf tube and flash-frozen in liquid nitrogen. Subsequently, the concentrations of IL-10 and IL-1β in these samples were determined using commercially available rat-specific enzyme-linked immunosorbent assay (ELISA) kits (My-Biosource, Inc., San Diego, CA, USA; MBS2020828 [detection range of 7.8-500 pg/mL and sensitivity of<3.5 pg/mL] and MBS2023030 [detection range of 15.6-1000 pg/mL and sensitivity of<5.4 pg/mL]), following the protocols provided by the manufacturer.

Qualitative histopathological assessments

After CSF collection, two rats in each group were randomly selected for qualitative histopathological assessments. For histopathological analysis, brain tissue was collected from each experimental group following euthanasia. Euthanasia was induced using an intraperitoneal injection of sodium thiopental (20 mg per 100 g of body weight, from a 60 mg/mL solution). Subsequently, the rats underwent transcardial perfusion, with 0.9% saline, followed by 4% paraformaldehyde. The brains were then extracted and post-fixed by immersion in 10% buffered formalin for 48 hours at room temperature. After fixation, the tissue samples were dehydrated through a graded ethanol series, cleared in xylenol, and finally embedded in paraffin blocks. Using a microtome, sequential 5-µm thick coronal sections were prepared and stained with hematoxylin and eosin (H&E) for examination. The analysis focused primarily on the CA1 area of the hippocampus. Hippocampal sections were specifically obtained from the dorsal hippocampus at the stereotaxic coordinates -4.56 mm from bregma, with a depth and laterality of 3.5 mm.

Cerebral edema assessment

Brain edema was calculated on the remaining six rats in each group using a formula derived from prior research (Rahimi et al., 2021) (Equation 1):

1. Cerebral edema percentage (brain water content [BWC])=×100

Statistics

Statistical analyses were conducted using GraphPad Prism software, version 8. Quantitative data were assessed for normality. Provided that assumptions were met, comparisons across groups were performed using repeated-measures analysis of variance (ANOVA), followed by one-way ANOVA. When applicable, the Newman-Keuls post hoc test was employed. For all two-sided comparisons, Tukey's post hoc test was applied where appropriate. The results are expressed as the Mean±SEM. A probability value of P≤0.05 was considered statistically significant.

Results

Efficacy of ATX on neurological function, motor and balance function, and spatial memory

The MCAO and DMSO (solvent) groups demonstrated markedly elevated Bederson scores relative to the intact and sham groups (P<0.001). Administration of low and medium doses of ATX resulted in a significant reduction of these neurological deficit scores compared to the MCAO and solvent groups (P<0.001 and P<0.01, respectively). In contrast, the high-dose quality control (QC) group showed no statistically significant improvement (Figure 2A).

A similar pattern was observed in the rotarod test, where latency to fall was significantly longer in the low- and medium-dose ATX groups than in the untreated MCAO and DMSO controls (P<0.001 and P<0.01, respectively). Again, the high-dose group's performance did not differ significantly (Figure 2B).

Regarding rats' performance on the shuttle box test, no significant differences were observed in the number of acquisition trials across the experimental groups (Figure 2C). The analysis indicated that animals receiving low and medium ATX doses demonstrated a statistically significant enhancement in both the duration spent in the dark compartment (Figure 2D) and STL (Figure 2E). Conversely, the high-dose treatment group failed to exhibit any significant improvements in these metrics relative to controls.

Efficacy of ATX on spatial learning results in the MWM test

In the MWM, rats treated with low and medium concentrations of ATX exhibited significantly better spatial learning and memory than the MCAO and DMSO (Solvent) groups. This was evidenced by shorter latencies to find the hidden platform (Figure 3A), a shorter total path length to the platform (Figure 3 B), more time spent in the target quadrant (Figure 3C), and a higher frequency of entries into the correct quadrant (Figure 3D). No significant cognitive enhancement was detected in the high-dose group.

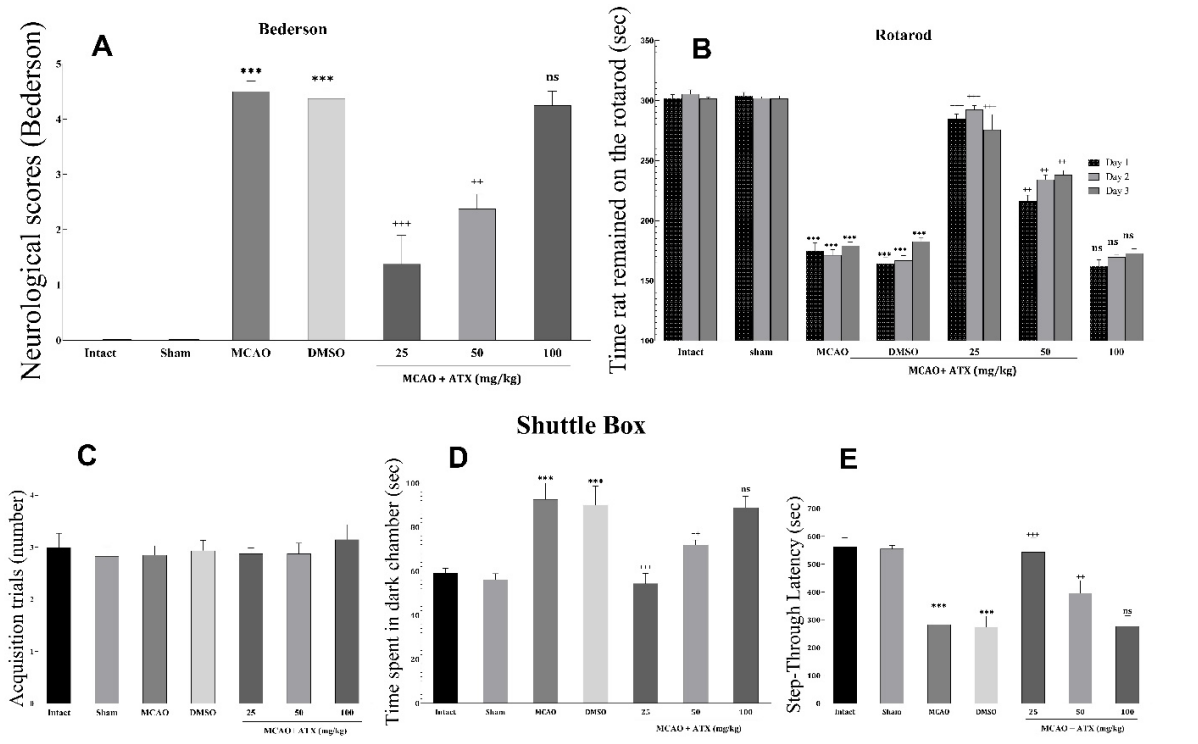

Figure 2. Results of neurobehavioral and functional tests

A) Bederson neurologic scores, B) The time rats to remain and keep balance on the rotarod device, Shuttle box spatial memory test results: C) The number of trials required for learning in the shuttle box, D) The time spent in the dark chamber, E) The time duration rats stayed in the light chamber before entering the darkroom (step-through)

Ns: Not significant.

$^{***}P<0.001$, $^{+}P<0.05$, $^{++}P<0.01$, $^{+++}P<0.001$.

Efficacy of ATX on IL levels

The analysis of cytokine levels showed that the low- and medium-dose groups exhibited a significantly elevated IL-10 concentration along with a markedly reduced IL-1β level compared to the MCAO and DMSO (solvent) control groups. In contrast, no significant alterations in either IL were detected in the high-dose group (Figure 4).

Efficacy of ATX on cerebral edema

Cerebral edema, measured by BWC, was markedly elevated in the MCAO and DMSO (solvent) groups compared to the intact and sham controls ($P<0.001$), confirming a rise in edema following stroke induction. Treatment with low and medium doses of ATX significantly reduced BWC ($P<0.001$ and $P<0.01$, respectively). Low dosage demonstrated the most potent effect in mitigating edema. Conversely, the group administered the high dose of ATX showed no statistically significant difference from the stroke control groups (Figure 5).

Qualitative histopathological assessments of ATX neuroprotective effects on hippocampal CA1 region

As shown in Figure 6, the control groups without induced stroke (A, B) show normal neuronal cytoarchitecture, with distinct nuclei and no signs of apoptosis. Conversely, the stroke model groups (C, D) demonstrated extensive cellular damage, including pronounced pyknotic nuclei and condensed chromatin. ATX administration at 25 mg/kg (E) and 50 mg/kg (F) promoted notable neuronal recovery, with most cells displaying near-normal morphology and clear nuclei, despite some residual apoptotic cells. In contrast, the 100 mg/kg ATX (G) dosage did not confer a significant protective effect, as tissue morphology was comparable to that of the untreated stroke groups.

Discussion

This study aimed to examine the neuroprotective potential of ATX following MCAO in rats. The results in-

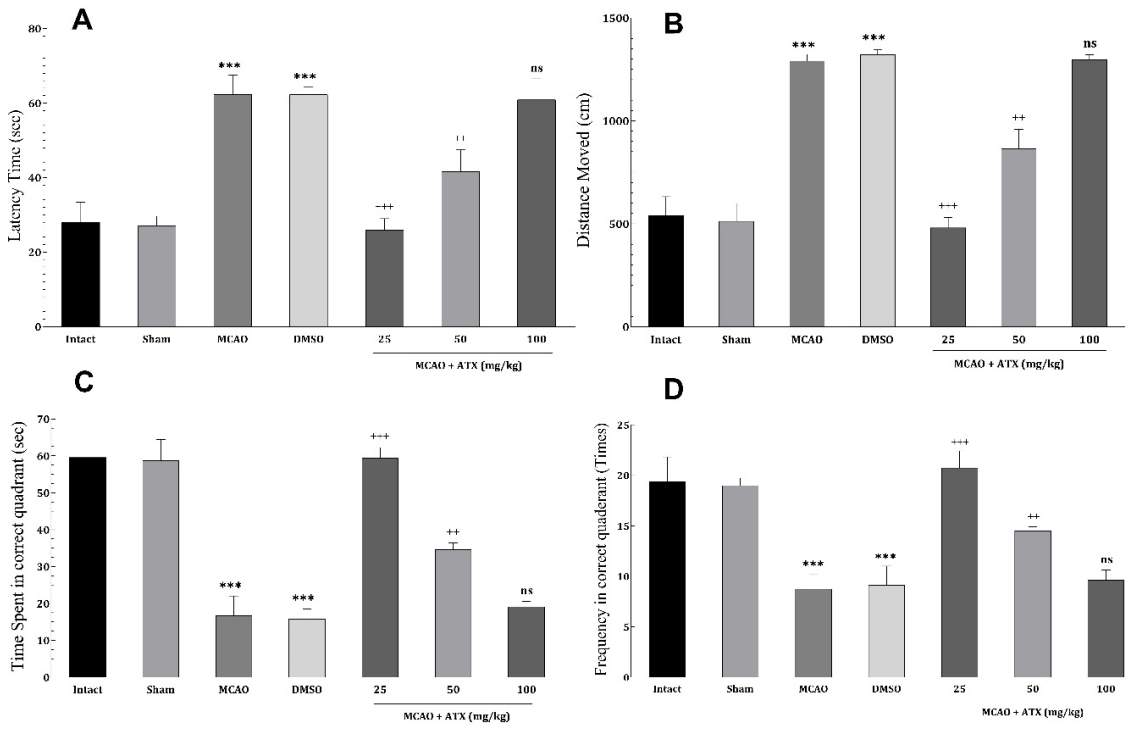

Figure 3. MWM test results

A) The time taken by the rats to reach the hidden platform, B) The distance traveled to reach the hidden platform, C) The total time duration rats spent in the correct quadrant, D) The number of times rats present in the correct quadrant

Ns: Not significant.

$^{***}P<0.001$, $^{+}P<0.05$, $^{++}P<0.01$, $^{+++}P<0.001$.

dicated that ATX at doses of 25 and 50 mg/kg conferred significant protection, as evidenced by improved neurobehavioral and functional outcomes, reduced cerebral edema, and enhanced histological preservation (with the lower dose demonstrating the greatest improvements). However, these beneficial effects were not observed at the higher dose of 100 mg/kg, suggesting a loss of efficacy.

ATX demonstrates robust neuroprotective effects against cerebral ischemia/reperfusion (I/R) injury, as evidenced by consistent improvements in neurological function, reduced infarct volume, and decreased neuronal loss in various animal models. Its efficacy is observed with both pre- and post-I/R administration, via oral or intraperitoneal routes, across a wide dose range. The protective mechanisms are multifaceted, primarily involving potent antioxidant activity through the upregulation of the Nrf2/HO-1 signaling pathway and key enzymes, such as superoxide dismutase (SOD) and catalase (CAT), leading to reduced oxidative stress markers (Park, 2025; Wang & Qi, 2022). ATX upregulates the cellular antioxidant defense system by activating the Nrf2 signaling pathway. This activation, potentially mediated through the phosphatidylinositol 3-kinase/protein kinase B PI3K/Akt and signal-regulated kinase (ERK) pathways, which inhibit glycogen synthase kinase-3 beta (GSK3β), leads to the transcription of cytoprotective genes, such as HO-1, bolstering the brain's resistance to oxidative stress (Wang & Qi, 2022; Wang et al., 2024). Recent studies have confirmed that ATX treatment in cerebral IR models restores glutathione (GSH) levels and SOD activity while significantly reducing malondialdehyde (MDA) levels, a key marker of lipid peroxidation (Galasso et al., 2018).

ATX also exerts strong anti-apoptotic effects by modulating the balance between B-cell lymphoma-2 (Bcl-2) and Bax, inhibiting caspase activation, and protecting mitochondrial integrity. A critical neuroprotective effect of ATX is its ability to counter programmed cell death, including both apoptosis and parthanatos. It achieves this by increasing anti-apoptotic Bcl-2 and decreasing pro-apoptotic Bax, Caspase-3, and Cyt C, while also

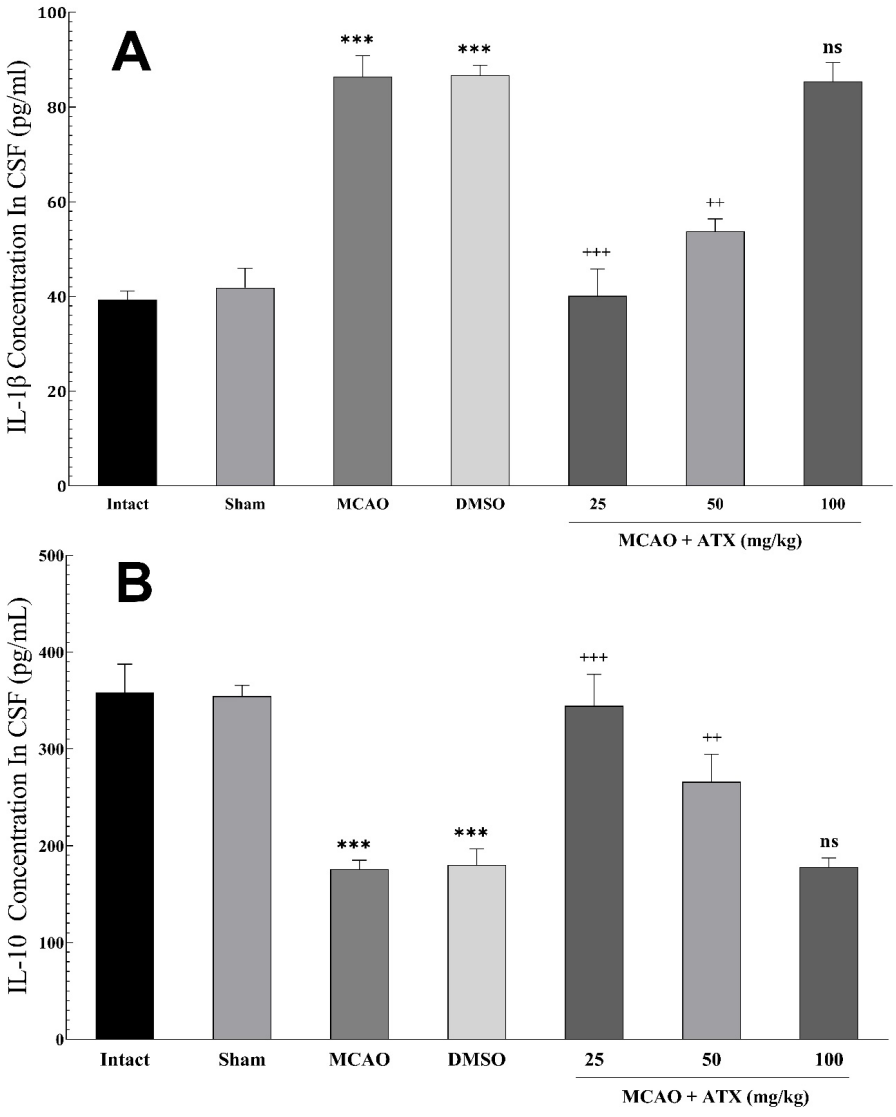

Figure 4. Concentration of ILs in the CSF

NEUROSCIENCE

A) Concentration of IL-1β in the CSF, B) Concentration of IL-10 in the CSF

Ns: Not significant.

$^{***}P<0.001$, $^{+}P<0.05$, $^{++}P<0.01$, $^{+++}P<0.001$.

modulating poly(ADP-ribose) polymerase 1 (PARP1) to prevent apoptosis-inducing factor (AIF)-mediated parthanatos (Wang et al., 2024). Furthermore, it protects neuronal cells from oxidative stress-induced apoptosis by suppressing mitochondrial abnormalities and the creation of intracellular ROS (Galasso et al., 2018).

Furthermore, it suppresses neuroinflammation by reducing pro-inflammatory cytokines, such as TNF-α, IL-6, or IL-1β (as indicated in the present study), and mitigates excitotoxicity by regulating glutamate levels. This is achieved primarily by suppressing the nuclear factor kappa-light-chain-enhancer of activated B cells (NF-κB) pathway through the inhibition of inhibitory kappa B kinase beta (IKKβ) phosphorylation and the nuclear translocation of the p65 subunit. Additionally, ATX inhibits the mitogen-activated protein kinase (MAPK) signaling pathways, including p38 and c-Jun N-terminal Kinase (JNK), further curtailing the neuroinflammatory response (Wang & Qi, 2022). Specifically, in activated microglial cells (BV-2 cell line), ATX drastically reduced the release of inflammatory mediators by modulating factors involved in the NF-κB cascade (e.g. phosphorylated IKKα [p-IKKα], p-IκBα, and p-NF-κB p65) and MAPK pathways (Galasso et al., 2018).

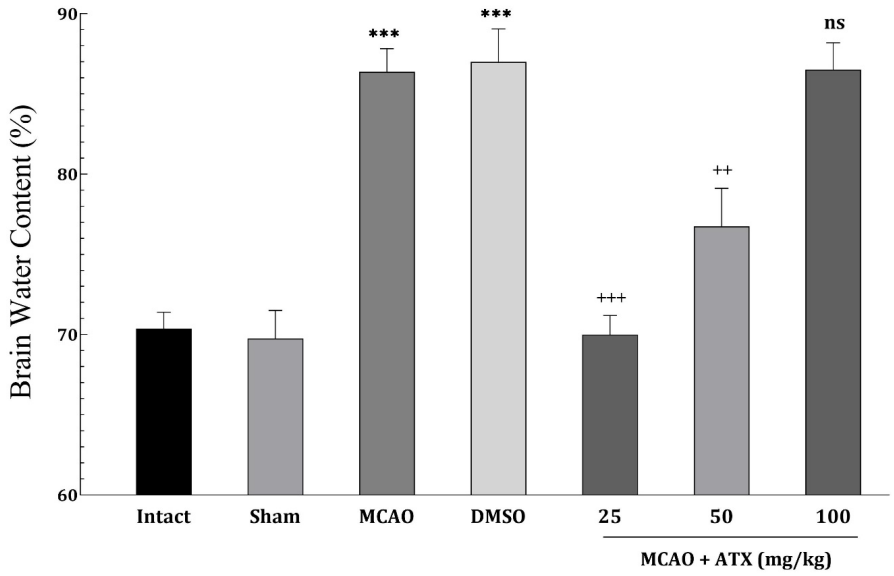

Figure 5. Cerebral edema presented as percentage of water in brain

NEUROSCIENCE

Ns: Not significant.

***P<0.001, +P<0.05, ++P<0.01, +++P<0.001.

Also, ATX modulates neuroinflammation by maintaining the integrity of the BBB, reducing brain edema, and preventing the infiltration of peripheral inflammatory cells into the central nervous system (CNS). ATX also protects the BBB by downregulating the astrocytic p75 neurotrophin receptor (p75NTR), leading to increased expression of tight junction proteins ZO-1 and claudin-5, thereby preserving BBB integrity and reducing the risk of hemorrhagic transformation (Wang et al., 2024). It also exhibits systemic anti-inflammatory properties, alleviating peripheral inflammation, which can exacerbate neuroinflammation (Wang & Qi, 2022).

Additionally, ATX promotes neural regeneration and functional recovery by activating the cyclic adenosine monophosphate (cAMP)/protein kinase A (PKA)/cAMP-response element-binding protein (CREB) pathway and increasing the expression of growth factors, such as brain-derived neurotrophic factor (BDNF) and growth-associated protein 43 (GAP-43). Pre-treatment with ATX has been shown to promote nerve cell regeneration by increasing gene expression of GFAP (important for BBB function and repair), MAP-2 (for microtubule growth and neuronal regeneration), BDNF, and growth-associated protein 43 (GAP-43). It also promotes neurogenesis and improves behavioral performance in hippocampal-dependent tasks, which is a predominant mechanism for countering cognitive decline (Galasso et al., 2018). It also enhances DNA repair by reducing the DNA damage marker 8-OHdG and increasing the expression of the DNA repair protein PARP1 (116kDa), as well as upregulating NQO1 and Hsp70, which collectively help maintain genomic integrity and promote cell survival (Wang et al., 2024). A key feature enabling these neurological activities is its lipid-soluble nature, which allows it to cross the BBB and accumulate in brain regions such as the hippocampus and cerebral cortex (Si & Zhu, 2022). It is important to note that natural ATX (from sources, such as *Haematococcus pluvialis*) is esterified, which confers higher bioavailability compared to the synthetic, unesterified version, making the natural form significantly superior in its antioxidant and anti-inflammatory properties (Galasso et al., 2018).

Similar to our study, Taheri et al. (2022) investigated the dose-dependent effects of on I/R-induced brain injury in a rat MCAO model. ATX administration, particularly at the medium dose of 45 mg/kg, significantly reduced stroke volume and improved neurological sensorimotor deficits. Mechanistically, ATX demonstrated potent antioxidant properties by reducing lipid peroxidation and restoring total oxidant status and GSH levels to normal levels. It enhanced the activity of the antioxidant enzyme glutathione peroxidase (GPX). It increased the gene expression of key antioxidant enzymes, including CAT, SOD, and GPX, which were suppressed after ischemia. A significant and novel finding was ATX's pronounced upregulation of the glutamate transporter (GLT-1) (excitatory amino acid transporter 2 [EAAT2]), which is

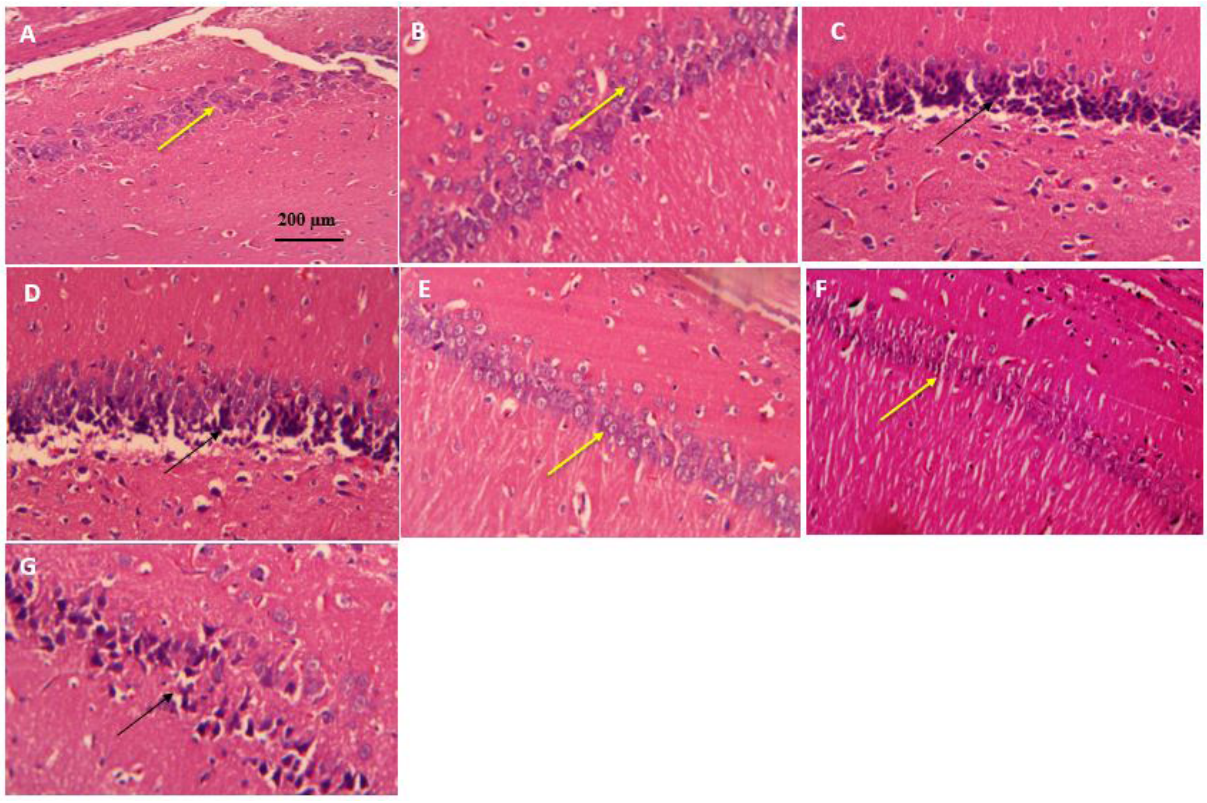

Figure 6. Qualitative histopathological assessment of the hippocampal CA1 region using H&E staining and magnification of 200x

A) Intact, B) Sham, C) MCAO, D) Vehicle, E) ATX 25 mg/kg, F) ATX 50 mg/kg, G) ATX 100 mg/kg

Note: Yellow arrows indicate normal neurons. Black arrows indicate necrotic neurons.

crucial for clearing excess synaptic glutamate and preventing excitotoxicity. The study concluded that the 45 mg/kg dose was most effective for the primary endpoints of stroke volume and neurological function, highlighting the importance of timing of administration (acutely after occlusion and before reperfusion).

Both studies found a clear relationship between ATX administration and consequent improved outcomes (function, edema, anti-inflammation). These effects were observed in Taheri et al.'s study with a single acute dose, while we studied a repeated-dosing protocol (Taheri et al., 2022). This is a critical difference. The ineffectiveness of our 100 mg/kg dose, compared with Taheri's 65 mg/kg dose, strongly suggests that dosing frequency and cumulative exposure are crucial. Our regimen resulted in a much higher total ATX exposure (6 doses of 100 mg/kg vs one dose of 65 mg/kg). It is plausible that very high, repeated doses may lead to receptor saturation, feedback inhibition, or even pro-oxidant effects, explaining the loss of efficacy observed. This highlights a path for future studies.

Xue et al. (2017) demonstrated that ATX treatment ameliorated learning and memory deficits in a mouse model of vascular cognitive impairment induced by repeated cerebral ischemia/reperfusion. The study found that ATX administration rescued the loss of pyramidal neurons in the hippocampal CA1 and CA3 regions. Mechanistically, ATX decreased oxidative stress, as evidenced by reduced MDA and increased antioxidants GSH and SOD. Furthermore, ATX reduced ultrastructural damage to neurons and mitochondria observed via electron microscopy. The anti-apoptotic effect of ATX was confirmed by modulating key proteins. ATX decreased the expression of pro-apoptotic proteins, including cytochrome C, cleaved caspase-3, and Bax, while increasing the expression of the anti-apoptotic protein Bcl-2. The study concluded that ATX protects against cognitive deficits and neuronal damage primarily by attenuating oxidative stress and subsequent apoptosis.

We used a focal ischemia model (transient MCAO), which mimics a localized stroke, such as an embolic clot in a major cerebral artery. However, Xue et al. (2017)

used a global ischemia model (repeated bilateral CCA occlusion [BCCAO]), which induces widespread cerebral hypoperfusion and is a model for vascular cognitive impairment. We employed a repeated-dosing protocol (IP injection every 12 hours for 3 days, 6 total doses) across a range of doses (25, 50, 100 mg/kg); however, Xue et al. (Xue et al., 2017) used a single, lower dose (10 mg/kg) administered daily via intragastric gavage for a much longer duration (28 days). This is a critical difference. Our study's investigation of multiple doses and the discovery of an inverted dose-response curve is a significant advancement and identifies a potential therapeutic window for ATX, which was not explored in the study by Xue et al. (2017).

Park et al. (2022) investigated the neuroprotective effects of ATX against severe I/R injury in the forebrain of gerbils. The model used was a 15-minute transient bilateral CCA occlusion, which induces massive, delayed neuronal death across the hippocampal CA1-3 regions. The research employed a pre-treatment protocol, administering a high dose of ATX (100 mg/kg, intraperitoneally) once daily for three consecutive days prior to ischemia induction. The key findings were that ATX pre-treatment significantly attenuated the severe I/R-induced loss of pyramidal neurons in the hippocampal CA1-3 areas, as confirmed by Nissl staining, NeuN immunohistochemistry, and reduced Fluoro-Jade B staining (a marker for neuronal degeneration). The proposed mechanism for this neuroprotection was a potent reduction in oxidative stress. This was evidenced by ATX's ability to significantly decrease immunoreactivity for markers of oxidative DNA damage (8OHdG) and lipid peroxidation (4-hydroxynonenal [4HNE]) in the hippocampal neurons one day after I/R. Furthermore, ATX pre-treatment itself boosted the baseline levels of the key antioxidant enzymes SOD1 and SOD2 in the hippocampus and helped maintain their expression after I/R, which was otherwise significantly reduced in the untreated I/R group. The study concluded that ATX confers neuroprotection against severe ischemic brain injury primarily through its robust antioxidant activity, which mitigates oxidative damage to cellular components.

Our study used a focal ischemia model in rats (transient MCAO), which mimics a localized stroke, such as an embolic clot blocking a major cerebral artery; however, Park et al. (2022) used a global forebrain ischemia model in gerbils (15-minute bilateral CCA occlusion), which mimics conditions, such as cardiac arrest, leading to widespread hippocampal damage. Our rat MCAO model is more clinically relevant for the most common type of human stroke. Additionally, we employed a post-treatment, repeated-dosing protocol (25, 50, 100 mg/kg, IP, 30 minutes after MCAO and every 12 hours for 3 days). The most significant finding was an inverted dose-response, where 25 and 50 mg/kg were effective, but 100 mg/kg lost all efficacy; however, Park et al. (2022) employed a pre-treatment protocol with a high dose regimen (100 mg/kg, IP, once daily for 3 days before ischemia), which was highly effective in providing neuroprotection. This is the most critical difference. The core of the discrepancy lies not in the dose itself, but in the interaction between the dose, the dosing regimen, and the pathological context. Administering ATX before the ischemic insult acts as a pharmacological preconditioning agent; thus, when the severe ischemia hits, the brain is already in a heightened state of defense, allowing it to better withstand the oxidative burst upon reperfusion (as in the study by Park et al.). On the other hand, in a post-treatment approach, the injury cascade (excitotoxicity, oxidative stress, and inflammation) was already initiated by the time the first dose was administered 30 minutes post-MCAO (as in our study). In this context, a single high dose might be beneficial, but repeated high doses (six injections of 100 mg/kg) in an already compromised brain may overwhelm or disrupt the very pathways you are trying to activate. Future studies should be designed to directly test this hypothesis. Future studies can use identical high (100 mg/kg) and medium (50 mg/kg) doses of ATX, but administer them in different temporal regimens: Pre-ischemia only, post-ischemia only (as in your study), or a combination of both. Compare outcomes to pinpoint the critical window and interaction with injury progression.

Lu et al. (2010) demonstrated that ATX pre-treatment provides significant neuroprotection against cerebral I/R injury. In their in vivo rat MCAO model, intragastric administration of ATX (50 and 80 mg/kg) prior to ischemia dramatically reduced infarct volume and improved neurological scores in a dose-dependent manner, with 80 mg/kg being the most effective. Histological analysis via Nissl staining confirmed that ATX reduced neuronal loss. The proposed mechanism is primarily rooted in its potent antioxidant activity. Their in vitro experiments showed that ATX attenuated H_2O_2-induced cytotoxicity and apoptosis in cortical neurons and restored the mitochondrial membrane potential, suggesting the mitochondrial pathway is key to its protective effect. The study concluded that ATX's free radical scavenging activity and its ability to enhance membrane stability are central to its neuroprotective properties. In another study by Yegin et al. (2023), the neuroprotective and antioxidant roles of ATX were further supported in a cerebral ischemia-reperfusion model. They found that pre-ischemic

IP administration of ATX (25 and 75 mg/kg) significantly mitigated oxidative stress. This was evidenced by a dose-dependent increase in the activity of antioxidant enzymes SOD and CAT and a decrease in the lipid peroxidation marker MDA, with the high dose (75 mg/kg) showing the strongest effect, even bringing MDA below control levels. Histologically, both ATX doses reduced neuronal necrosis and damage in the cerebral cortex compared to the sham group, indicating a tangible neuroprotective effect.

Out study revealed a clear inverted dose-response curve. The low (25 mg/kg) and medium (50 mg/kg) doses were highly effective, while the high dose (100 mg/kg) showed no significant benefit across all parameters. However, Lu et al. (2010) and Yegin et al. (2023) both reported a linear or positive dose-response within their tested ranges, where a higher dose conferred greater protection. This is the most critical difference and is likely due to the dosing regimen. Our study used a post-treatment, repeated-dosing protocol (6 doses over 3 days), resulting in a much higher cumulative exposure (600 mg/kg total for the high-dose group). In contrast, Lu et al. (2010) and Yegin et al. (2023) used a single, pre-ischemic dose.

Similarly, Pan et al. (2017) used a preventive, pre-treatment protocol (oral administration for 7 days before MCAO). They reported a linear or positive dose-response, with a higher dose (10 mg/kg) being more effective than a lower one (5 mg/kg). Shen et al. (2009) used a single, acute pre-treatment dose administered directly into the brain (interacerebroventricular) just before MCAO. While the stroke models are similar, the route of administration differs between studies. Ours IP and Pan's oral routes are more clinically translatable than the intracerebroventricular (ICV) route used by Shen et al. (2009). Nevertheless, the consistent effects across oral, IP, and ICV routes strengthen the evidence for ATX's efficacy, provided that the dosing regimen is appropriate.

Future research should systematically investigate the therapeutic window for ATX administration and determine the optimal time post-stroke for intervention. Furthermore, studies should explore the effects of chronic, lower-dose administration to align with practical clinical scenarios for secondary prevention or recovery. The stark difference in efficacy between pre-treatment and our post-treatment, repeated-dosing regimen highlights the need to understand the pharmacodynamics of ATX in the dynamically changing post-ischemic brain environment. To robustly bridge the gap between these promising preclinical results and human trials, future work should adhere to established translational guidelines, such as the stroke therapy academic industry roundtable (STAIR) recommendations, including but not limited to the following:

Confirming efficacy in higher-order species (e.g. non-human primates) with more human-like brain anatomy.

Assessing recovery over weeks or months to ensure sustained benefit and functional relevance.

Investigating ATX in conjunction with existing recanalization therapies (such as tPA or thrombectomy) to model real-world clinical use and assess for synergistic effects.

Developing clinically viable formulations (e.g. for intravenous administration in acute settings) and conducting detailed pharmacokinetic and toxicological studies to define safe dosing parameters in humans.

Conclusion

In conclusion, this study demonstrates that ATX, administered post-ischemia, confers significant neuroprotection in a rat focal transient MCAO model. The 25 and 50 mg/kg doses effectively improved neurological and cognitive function, reduced cerebral edema, modulated the neuroinflammatory response by increasing IL-10 and decreasing IL-1β, and preserved the histological integrity of vulnerable hippocampal CA1 neurons, with the lower 25 mg/kg dose demonstrating the most beneficial effects. The most salient finding, however, is the loss of therapeutic efficacy at the higher dose of 100 mg/kg, revealing a distinct inverted dose-response relationship. This underscores that the neuroprotective benefits of ATX are critically dependent on dosing regimen and timing relative to the ischemic insult. These findings position ATX as a promising candidate for stroke therapy but necessitate careful, systematic future investigation to delineate its optimal clinical application window and dosage to harness its full therapeutic potential while avoiding the loss of effect at higher exposures.

Ethical Considerations

Compliance with ethical guidelines

This study was approved by the Research Ethics Committee of Laboratory Animals, Mazandaran University of Medical Sciences, Sari, Iran (Code: IR.MAZUMS.AEC.1403.031). All procedures performed in this study were in accordance with the animal research: Report-

ing of in vivo experiments (ARRIVE) guidelines and the ethical standards of the Institutional Research Ethics Committee of Mazandaran University of Medical Sciences, and in accordance with the Guidance on the Operation of Animals (Scientific Procedures) Act 1986 and associated guidelines.

Funding

Partial financial support for this project was provided by Mazandaran University of Medical Sciences, Sari, Iran (Grant No.: 18994).

Authors' contributions

Conceptualization: Ali Siahposht-Khachaki and Erfan Ghadirzadeh; Methodology, resources, and supervision: Ali Siahposht-Khachaki; Data curation: Parsa Pourmohammadi, Mobina Gheibi, and Melika Pourhossein; Formal analysis: Ali Siahposht-Khachaki and Sina Baghi Keshtan; Project administration: Ali Siahposht-Khachaki, Parsa Pourmohammadi, Mobina Gheibi, and Melika Pourhossein; Software: Ali Siahposht-Khachaki, Erfan Ghadirzadeh, and Sina Baghi Keshtan; Validation: Erfan Ghadirzadeh and Ali Siahposht-Khachaki; Visualization: Erfan Ghadirzadeh, Mobina Gheibi, and Sina Baghi Keshtan; Writing the original draft: Mobina Gheibi, Erfan Ghadirzadeh, and Sina Baghi Keshtan; Review and editing: All authors.

Conflict of interest

The authors declared no conflict of interest.

Acknowledgments

The authors thank the Deputy of Research and Technology of Mazandaran University of Medical Sciences for partially funding this study.

References

Ashrafizadeh, M., Ahmadi, Z., Yaribeygi, H., Sathyapalan, T., & Sahebkar, A. (2022). Astaxanthin and Nrf2 signaling pathway: A novel target for new therapeutic approaches. *Mini Reviews in Medicinal Chemistry, 22*(2), 312-321. [DOI:10.2174/1389557521666210505112834] [PMID]

Bieber, M., Gronewold, J., Scharf, A. C., Schuhmann, M. K., Langhauser, F., & Hopp, S., et al. (2019). Validity and reliability of neurological scores in mice exposed to middle cerebral artery occlusion. *Stroke, 50*(10), 2875-2882. [DOI:10.1161/STROKEAHA.119.026652] [PMID]

Brendler, T., & Williamson, E. M. (2019). Astaxanthin: How much is too much? A safety review. *Phytotherapy Research, 33*(12), 3090-3111. [DOI:10.1002/ptr.6514] [PMID]

Galasso, C., Orefice, I., Pellone, P., Cirino, P., Miele, R., & Ianora, A., et al. (2018). On the neuroprotective role of astaxanthin: New perspectives? *Marine Drugs, 16*(8), 247. [DOI:10.3390/md16080247] [PMID]

Grimmig, B., Kim, S. H., Nash, K., Bickford, P. C., & Douglas Shytle, R. (2017). Neuroprotective mechanisms of astaxanthin: A potential therapeutic role in preserving cognitive function in age and neurodegeneration. *Geroscience, 39*(1), 19-32. [DOI:10.1007/s11357-017-9958-x] [PMID]

Jurcau, A., & Ardelean, A. I. (2022). Oxidative stress in ischemia/reperfusion injuries following acute ischemic stroke. *Biomedicines, 10*(3), 574. [DOI:10.3390/biomedicines10030574] [PMID]

Li, S., Takahara, T., Fujino, M., Fukuhara, Y., Sugiyama, T., & Li, X. K., et al. (2017). Astaxanthin prevents ischemia-reperfusion injury of the steatotic liver in mice. *Plos One, 12*(11), e0187810. [DOI:10.1371/journal.pone.0187810] [PMID]

Liang, H., Kurimoto, S., Shima, K. R., Ota, T., Minabe, Y., & Yamashima, T. (2016). Why is hippocampal CA1 especially vulnerable to ischemia. *SOJ Biochem 2*(2), 7. [DOI:10.15226/2376-4589/2/2/00114]

Lin, L., Wang, X., & Yu, Z. (2016). Ischemia-reperfusion injury in the brain: mechanisms and potential therapeutic strategies. *Biochemistry & Pharmacology: Open Access, 5*(4), 213. [DOI:10.4172/2167-0501.1000213] [PMID]

Lu, Y. P., Liu, S. Y., Sun, H., Wu, X. M., Li, J. J., & Zhu, L. (2010). Neuroprotective effect of astaxanthin on H(2)O(2)-induced neurotoxicity in vitro and on focal cerebral ischemia in vivo. *Brain Research, 1360,* 40–48. [DOI:10.1016/j.brainres.2010.09.016] [PMID]

Mahyar, M., Ghadirzadeh, E., Nezhadnaderi, P., Moayedi, Z., Maboud, P., & Ebrahimi, A., et al. (2025). Neuroprotective effects of quercetin on hippocampal CA1 neurons following middle cerebral artery ischemia-reperfusion in male rats: A behavioral, biochemical, and histological study. *BMC Neurology, 25*(1), 9. [DOI:10.1186/s12883-024-04017-z] [PMID]

Nunez, J. (2008). Morris water maze experiment. *Journal of visualized experiments: JoVE, (19),* 897. [DOI:10.3791/897] [PMID]

Othman, M. Z., Hassan, Z., & Che Has, A. T. (2022). Morris water maze: A versatile and pertinent tool for assessing spatial learning and memory. *Experimental Animals, 71*(3), 264-280. [DOI:10.1538/expanim.21-0120] [PMID]

Otsuka, T., Shimazawa, M., Inoue, Y., Nakano, Y., Ojino, K., & Izawa, H., et al. (2016). Astaxanthin protects against retinal damage: evidence from in vivo and in vitro retinal ischemia and reperfusion models. *Current Eye Research, 41*(11), 1465-1472. [DOI:10.3109/02713683.2015.1127392] [PMID]

Pan, L., Zhou, Y., Li, X. F., Wan, Q. J., & Yu, L. H. (2017). Preventive treatment of astaxanthin provides neuroprotection through suppression of reactive oxygen species and activation of antioxidant defense pathway after stroke in rats. *Brain Research Bulletin, 130,* 211-220. [DOI:10.1016/j.brainresbull.2017.01.024] [PMID]

Park, J. H. (2025). Neuroprotective bioactive compounds from marine algae and their by-products against cerebral ischemia-reperfusion injury: A comprehensive review. *Applied Sciences, 15*(19), 10791. [DOI:10.3390/app151910791]

Park, J. H., Lee, T. K., Kim, D. W., Ahn, J. H., Lee, C. H., & Kim, J. D., et al. (2022). Astaxanthin confers a significant attenuation of hippocampal neuronal loss induced by severe ischemia-reperfusion injury in gerbils by reducing oxidative stress. *Marine Drugs, 20*(4), 267. [DOI:10.3390/md20040267] [PMID]

Qian, Y., Lu, X., Chen, L., Sun, J., Cao, K., & Yu, Q., et al. (2021). Effect of astaxanthin on neuron damage, inflammatory factors expressions and oxidative stress in mice with subarachnoid hemorrhage. *American Journal of Translational Research, 13*(11), 13043-13050. [PMID]

Qiu, X., Fu, K., Zhao, X., Zhang, Y., Yuan, Y., & Zhang, S.,et al. (2015). Protective effects of astaxanthin against ischemia/reperfusion induced renal injury in mice. *Journal of Translational Medicine, 13*(1), 28. [DOI:10.1186/s12967-015-0388-1] [PMID]

Rahimi, S., Dadfar, B., Tavakolian, G., Asadi Rad, A., Rashid Shabkahi, A., & Siahposht-Khachaki, A. (2021). Morphine attenuates neuroinflammation and blood-brain barrier disruption following traumatic brain injury through the opioidergic system. *Brain Research Bulletin, 176,* 103-111. [DOI:10.1016/j.brainresbull.2021.08.010] [PMID]

Saini, V., Guada, L., & Yavagal, D. R. (2021). Global epidemiology of stroke and access to acute ischemic stroke interventions. *Neurology, 97*(20_Supplement_2), S6-S16. [DOI:10.1212/WNL.0000000000012781] [PMID]

Shen, H., Kuo, C. C., Chou, J., Delvolve, A., Jackson, S. N., & Post, J., et al. (2009). Astaxanthin reduces ischemic brain injury in adult rats. *FASEB Journal, 23*(6), 1958-1968. [DOI:10.1096/fj.08-123281] [PMID]

Shimizu, K., Gupta, A., Brastianos, P. K., & Wakimoto, H. (2022). Anatomy-oriented stereotactic approach to cerebrospinal fluid collection in mice. *Brain Research, 1774,* 147706. [DOI:10.1016/j.brainres.2021.147706] [PMID]

Si, P., & Zhu, C. (2022). Biological and neurological activities of astaxanthin. *Molecular Medicine Reports, 26*(4), 300. [DOI:10.3892/mmr.2022.12816] [PMID]

Sun, M. S., Jin, H., Sun, X., Huang, S., Zhang, F. L., & Guo, Z. N., et al. (2018). Free radical damage in ischemia-reperfusion injury: An obstacle in acute ischemic stroke after revascularization therapy. *Oxidative Medicine and Cellular Longevity, 2018,* 3804979. [DOI:10.1155/2018/3804979] [PMID]

Taheri, F., Sattari, E., Hormozi, M., Ahmadvand, H., Bigdeli, M. R., & Kordestani-Moghadam, P., et al. (2022). Dose-dependent effects of astaxanthin on ischemia/reperfusion induced brain injury in mcao model rat. *Neurochemical Research, 47*(6), 1736-1750. [DOI:10.1007/s11064-022-03565-5] [PMID]

Themistoklis, K. M., Papasilekas, T. I., Melanis, K. S., Boviatsis, K. A., Korfias, S. I., & Vekrellis, K., et al. (2022). transient intraluminal filament middle cerebral artery occlusion stroke model in rats: A step-by-step guide and technical considerations. *World Neurosurgery, 168,* 43-50. [DOI:10.1016/j.wneu.2022.09.043] [PMID]

Wang, S., & Qi, X. (2022). The putative role of astaxanthin in neuroinflammation modulation: Mechanisms and therapeutic potential. *Frontiers in Pharmacology, 13,* 916653. [DOI:10.3389/fphar.2022.916653] [PMID]

Wang, X., Li, H., Wang, G., He, Z., Cui, X., & Song, F., et al. (2024). Therapeutic and preventive effects of astaxanthin in ischemic stroke. *Frontiers in Nutrition, 11,* 1441062. [DOI:10.3389/fnut.2024.1441062] [PMID]

Xue, Y., Qu, Z., Fu, J., Zhen, J., Wang, W., & Cai, Y., et al. (2017). The protective effect of astaxanthin on learning and memory deficits and oxidative stress in a mouse model of repeated cerebral ischemia/reperfusion. *Brain Research Bulletin, 131,* 221-228. [DOI:10.1016/j.brainresbull.2017.04.019] [PMID]

Yang, B. B., Zou, M., Zhao, L., & Zhang, Y. K. (2021). Astaxanthin attenuates acute cerebral infarction via Nrf-2/HO-1 pathway in rats. *Current Research in Translational Medicine, 69*(2), 103271. [DOI:10.1016/j.retram.2020.103271] [PMID]

Yeğin, B., Öz, S., Dönmez, D. B., Özden, H., Üstüner, M. C., & Kabay, S. C., et al. (2023). Effect of dose-related astaxanthin on rats with cerebral ischemia-reperfusion. *Yüksek İhtisas Üniversitesi Sağlık Bilimleri Dergisi, 4*(2), 42-49. [DOI:10.51261/yiu.2023.1350952]

Yuguang, Y., Changping, L., & Jiajia, H. (2025). Effects of astaxanthin on oxidative stress and inflammatory reaction in rats with traumatic brain injury based on Nrf2/HO-1 signaling pathway. *China Pharmacy, 34*(20), 2490-2496. [DOI:10.6039/j.issn.1001-0408.2023.20.08]

Zhu, H., Yoshimoto, T., Imajo-Ohmi, S., Dazortsava, M., Mathivanan, A., & Yamashima, T. (2012). Why are hippocampal CA1 neurons vulnerable but motor cortex neurons resistant to transient ischemia? *Journal of Neurochemistry, 120*(4), 574-585. [DOI:10.1111/j.1471-4159.2011.07550.x] [PMID]

This Page Intentionally Left Blank